JOURNAL OF MATERIALS SCIENCE 19 (1984) 3887–3894

The laser energy window for ion-implanted GaAs

M. A. SHAHID, B. J. SEALY, K. E. PUTTICK*
Department of Electronic and Electrical Engineering and
**Department of Physics, University of Surrey, Guildford, Surrey, UK*

A detailed study has been carried out of the energy window within which low resistivity, defect free, single crystal GaAs can be obtained following high dose implants of tin and selenium ions and laser annealing. A good correlation between electrical measurements, Rutherford backscattering and transmission electron microscopy has been obtained. The results indicate that there are four distinct bands of energy density corresponding to (i) an "amorphous" to polycrystalline transition accompanied by grain growth, (ii) the production of defective single crystal GaAs, (iii) the energy window and (iv) gross decomposition and laser induced damage.

1. Introduction

Published results [1, 2] for laser annealed, ion-implanted GaAs have shown that for a given implant condition a certain threshold energy density is required to crystallize the damaged layer and activate the implanted ions. Also, at higher energy densities the laser itself promotes decomposition of the surface. Within this energy window it is possible to get good electrical properties without severe decomposition.

Such an energy window has been discussed before for laser annealed silicon [3, 4]. For example, it has been shown that energy densities below the threshold value produce polycrystalline material with the crystallite size increasing with increasing energy density. Above the threshold energy density, crystalline material which is free of extended defects can be obtained. It has been demonstrated also that very high energy densities introduce damage and this can be used to getter impurities [5]. A similar study has been reported for tellurium-implanted GaAs [6] which shows that the threshold energy density necessary to recrystallize 0.23 μm is in excess of 1 J cm^{-2}. In contrast we have reported previously [7] that the threshold energy density is about 0.4 J cm^{-2} to recrystallize a similar thickness of damaged GaAs formed by an implant of 10^{15} Sn^{+}cm^{-2} at an energy of 300 keV. Perhaps the difference between these two sets of data is associated with the ions themselves, tellurium in one case and tin in the other. In the literature it is unclear as to the degree of decomposition of laser-irradiated GaAs and also the magnitude of the energy window [8]. Thus in an attempt to clarify the situation, we present in this paper the results of a detailed investigation of the energy window for tin and selenium implanted GaAs using electrical measurements, transmission electron microscopy (TEM) and Rutherford backscattering (RBS).

2. Experimental method

Tin and selenium ions were implanted at room temperature into (1 0 0) semi-insulating GaAs in a non-channelling direction. The ion doses were 5×10^{14} cm^{-2} and 1×10^{15} cm^{-2} and the ion energies were 100, 300 and 600 keV. The implanted specimens were cleaved into 2 mm x 2 mm squares for TEM studies and into 4 mm x 4 mm squares for electrical measurements. Annealing was carried out in air using a single 25 nsec pulse from a Q-switched ruby laser. An L-shaped quartz rod [9] was used to homogenize the energy density over an area of 6 mm in diameter. Foils for TEM analysis were prepared by thinning the specimens chemically from the back side only. The specimens were then examined in a JEOL 200 CX scanning transmission electron microscope (STEM) operated

0022–2461/84 $03.00 + .12

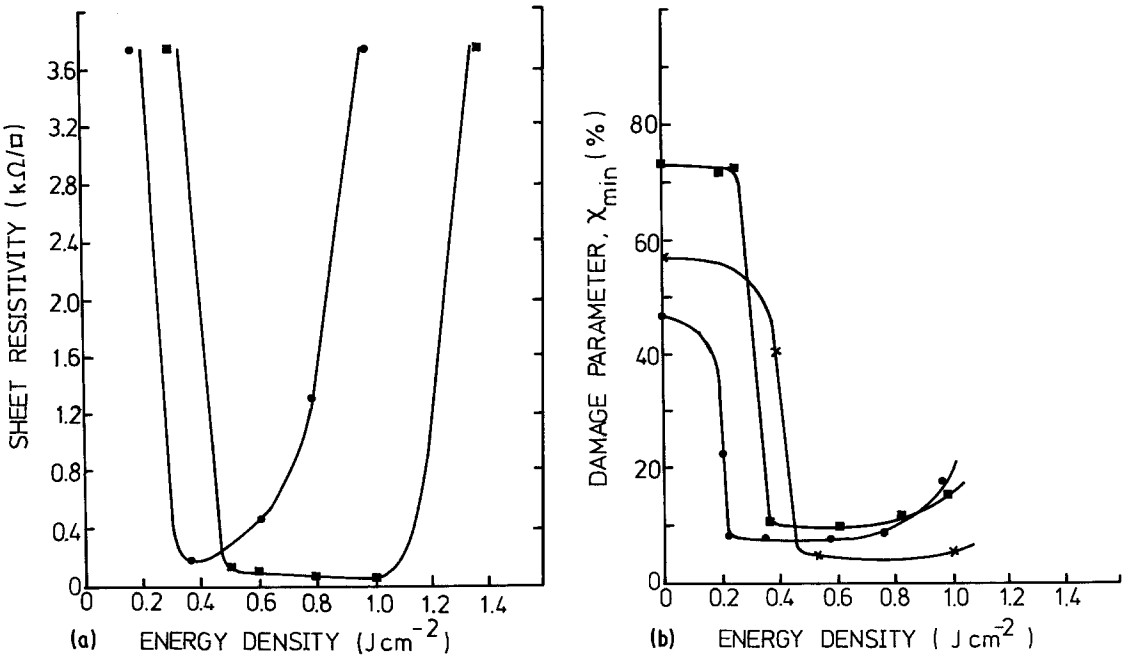

Figure 1 (a) Sheet resistivity as a function of energy density for selenium (▪) and tin (•) implanted GaAs (both 1×10^{15} ions cm^{-2} at 300 keV). (b) Damage parameter χ_{min} as a function of energy density for selenium (×) and tin implanted GaAs (100 keV tin •, 300 keV tin ▪, dose in all cases = 1×10^{15} ions cm^{-2}).

at 120 or 160 kV. The sheet resistivity was measured on clover-leaf specimens cut from 4 mm × 4 mm squares using the Van der Pauw technique. Electrical contact was made to these samples by alloying tin dots at about 250° C for 15 sec. Rutherford backscattering was carried out using the 1.5 MeV He^+ ions, the analysis area being 1 mm in diameter at the centre of the samples.

3. Results

3.1. Sheet resistivity

The sheet resistivity as a function of energy density was measured only for samples implanted with 1×10^{15} ions cm^{-2} at an energy of 300 keV (Fig. 1a). The thicknesses of the damage layers, measured by Rutherford backscattering, were 0.23 μm [7] and 0.26 μm for the tin and selenium implants, respectively. Thus slightly more energy should be required to melt through the damaged layer of the selenium implanted samples than for that of the tin implanted samples. In accord with this from Fig. 1a, the threshold energy densities to get good electrical properties are about 0.4 and 0.5 J cm^{-2} for selenium and tin implants, respectively.

The sheet resistivity for tin implanted samples increases with increasing energy density above 0.4 and at 1.0 J cm^{-2} is about 6000 Ω/□. In contrast the sheet resistivity for selenium implanted samples remains at a low value, less than 100 Ω/□, until irradiated with energy densities above 1.0 J cm^{-2}. Thus at energy densities above 1.0 J cm^{-2} both types of samples have very high resistivities.

3.2. Rutherford backscattering

The damage parameter, χ_{min}, which is the ratio of the yields behind the surface peaks in the aligned and random orientations, respectively, was determined as a function of energy density (see Fig. 1b). There is a marked decrease in the magnitude of χ_{min} with increasing energy density, low values of 5 to 10% being measured in the range 0.5 to 0.8 J cm^{-2}.

3.3. TEM

A set of micrographs for 100, 300 and 600 keV tin implants with a dose of 5×10^{14} ions cm^{-2} is shown in Figs. 2, 3 and 4, respectively. In all cases, the as-implanted samples had a thin surface layer consisting of a random distribution of extremely small crystalline particles*. This is evident from the dark

*This situation has been inappropriately referred to as "amorphous" in the literature.

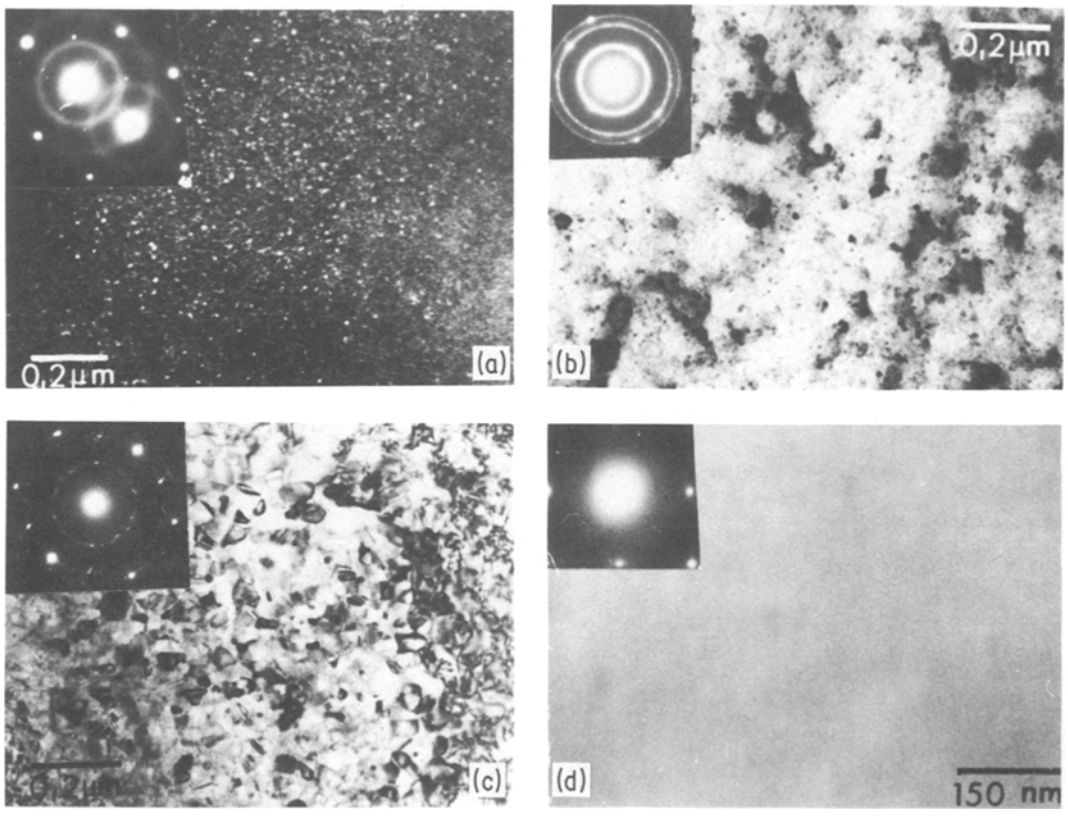

Figure 2 Transmission electron micrographs of laser annealed tin implanted GaAs. Ion dose = 5×10^{14} cm^{-2} and ion energy = 100 keV. (a) as-implanted, (b) 0.12 J cm^{-2}, (c) 0.20 J cm^{-2}, (d) 0.30 J cm^{-2}.

field micrograph of Fig. 2a which has been produced by tilting the electron beam such that a part of the first diffraction ring was aligned along the column axis of the microscope. The diffraction ring pattern superimposed on the spot pattern (in Figs. 2a and 3a) is a consequence of the fact that the electron beam was incident on the samples along the [1 0 0] direction, that is, first the beam passed through the single crystal substrate to produce the spot pattern and then left the sample through the implanted layer to give rise to the ring pattern. Moreover, a comparison of Figs. 2a, 3a and 4a shows that the crystalline particles in the as-implanted sample tend to increase in size with increasing ion energy for a given dose, probably due to self annealing during implantation.

The annealing process starts with growth of grains at the lower energy densities of the laser beam. With reference to Fig. 4, the grain growth occurs as the energy density is increased up to 0.6 J cm^{-2}. At 0.8 J cm^{-2}, the material is single crystal but contains large concentrations of dislocations, stacking faults and microtwins. However, irradiation at 1.0 J cm^{-2} produces defect free material. The same variation in defect structure with energy density can be seen for the 100 and 300 keV implants (Figs. 2 and 3) and these are summarized in Fig. 5. Thus we have identified four regions which depend on ion energy, that is, depend on the thickness of the damaged region following ion implantation. In the first region, the average grain size increases with increasing energy density (Fig. 6). It also shows that the threshold energy required to produce single crystal material increases with increasing ion energy (damage layer thickness). The second region (Fig. 5) corresponds to the production of defective crystalline GaAs and occurs over a narrow band of energy densities, the magnitude of which increases with increasing ion energy. This region is associated with the damaged layer just melting through, so that recrystallization is not perfect and takes place on somewhat defective GaAs, that is, on the tail of the damaged region.

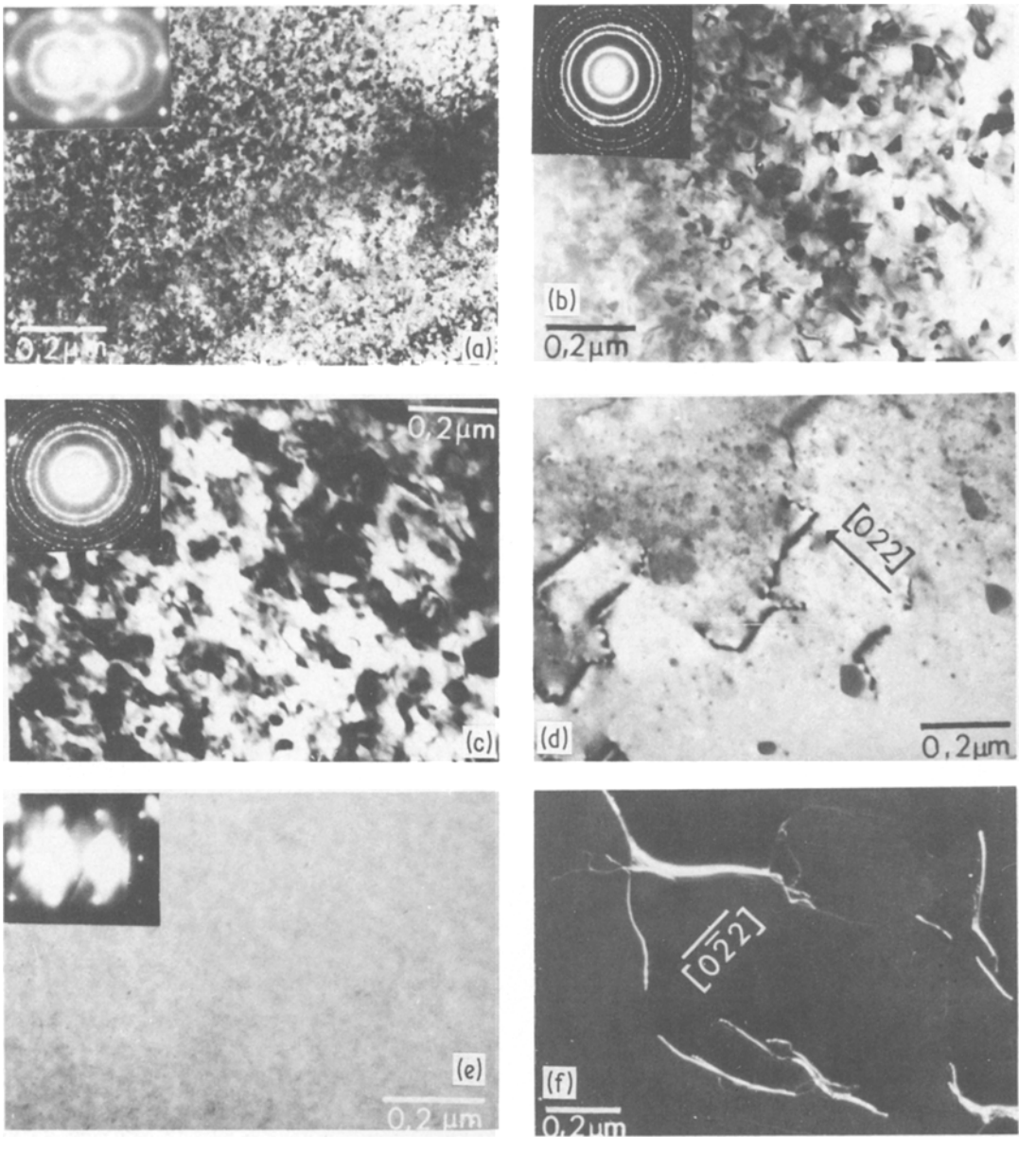

Figure 3 Transmission electron micrographs of laser annealed tin implanted GaAs. Ion dose = 5×10^{14} cm^{-2} and ion energy = 300 keV. (a) as-implanted, (b) 0.20 J cm^{-2}, (c) 0.30 J cm^{-2}, (d) 0.47 J cm^{-2}, (e) 0.70 J cm^{-2}, (f) 1.5 J cm^{-2}.

In situations where the defect density is comparatively low in this transition region, a detailed analysis of the nature of the defects has been carried out. For a 300 keV implant and a subsequent anneal at an energy density of 0.47 J cm^{-2}, the results are shown in Fig. 7, (note that Fig. 3d is the corresponding bright field image). The features worth noting are the dislocation lines, the small blobs (in Fig. 7a), the large blobs of dark contrast (in Fig. 3d) and the triangular features having fringes (compare the fringe spacings in Figs. 3d and 7a). Using $\mathbf{g} \cdot \mathbf{b}$ and $\mathbf{g} \cdot \mathbf{b} \wedge \mathbf{u}$ criteria, it has been found that the Burgers vectors of dislocation lines are $\frac{1}{2}\langle 1\,1\,0\rangle$ lying both in the specimen surface plane and inclined to it. The triangular fringed features have been observed by others [6] and thought to be stacking faults, but in this case they do not follow the contrast effects associated with stacking faults. They seem to be particles of second phase since they give rise to

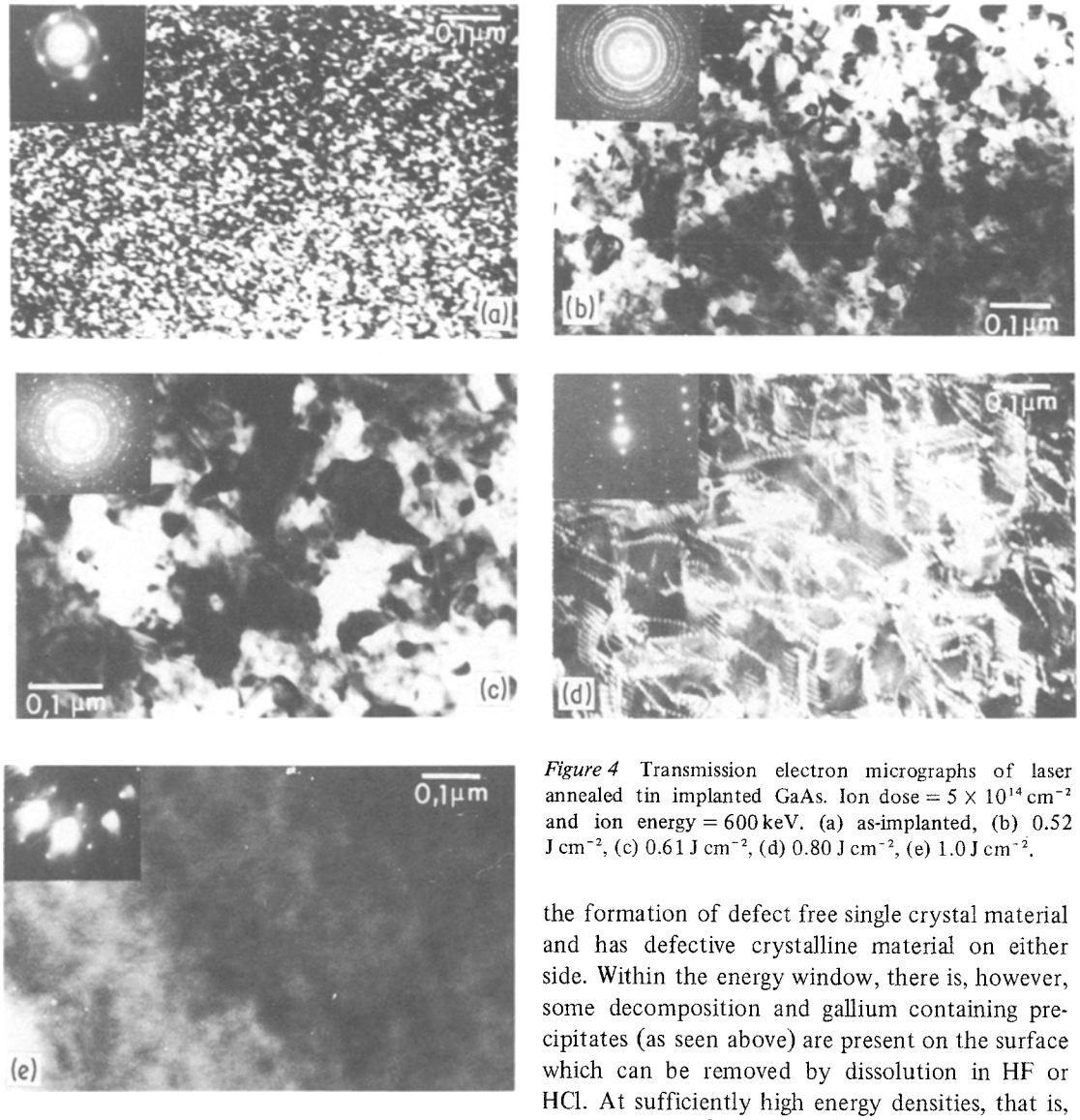

Figure 4 Transmission electron micrographs of laser annealed tin implanted GaAs. Ion dose = 5×10^{14} cm^{-2} and ion energy = 600 keV. (a) as-implanted, (b) 0.52 J cm^{-2}, (c) 0.61 J cm^{-2}, (d) 0.80 J cm^{-2}, (e) 1.0 J cm^{-2}.

extra diffraction spots around 2 0 0 and 2 2 0 spots (Fig. 7b) which are different from those arising from microtwins. Streaking in these spots is also clearly visible which is an indication of the strain experienced by the lattice. The bigger dark blobs lying on the surface (Fig. 3d) are due to gallium-rich precipitates which was established by micro-probing in the STEM. The other tiny areas of white contrast in Fig. 7a are believed to be due to implantation damage that lies near the tail of the implanted region, since stereo-microscopy shows that they lie deep within the sample. Under conditions of incomplete annealing, they become the sources of the defects described above.

The third region, the energy window, is due to the formation of defect free single crystal material and has defective crystalline material on either side. Within the energy window, there is, however, some decomposition and gallium containing precipitates (as seen above) are present on the surface which can be removed by dissolution in HF or HCl. At sufficiently high energy densities, that is, above 1.0 J cm^{-2}, the GaAs becomes damaged due to the action of the laser and contains a large density of dislocations and dislocation networks which become increasingly complex as the energy density is raised further. This is region 4. In addition, as a consequence of severe decomposition [2] above 1.0 J cm^{-2}, the specimen surface becomes very rough. In the extreme cracks form in the samples and eventually they disintegrate when the energy density is sufficiently high (i.e. > 2.5 J cm^{-2}) (Fig. 8).

4. Discussion

Although our previously published TEM results [10] were not carried out in such detail as those presented here, similar defect structures were

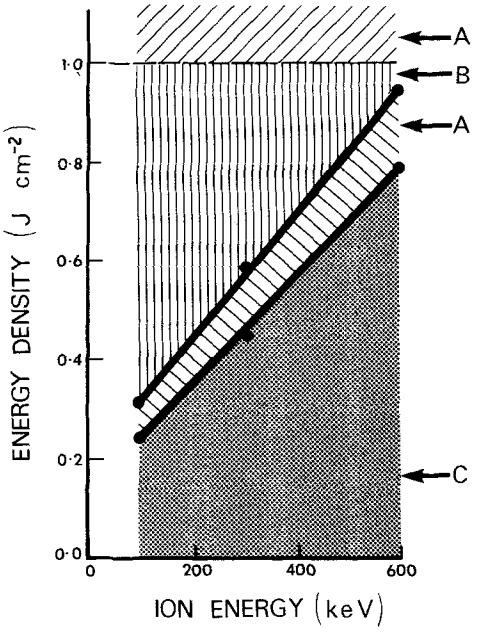

Figure 5 The energy window as a function of ion energy for 5×10^{14} Sn^+cm^{-2} implanted GaAs. Four distinct bands of energy density are shown. A – defective single crystal; B – defect free single crystal; C – polycrystalline.

observed for samples implanted with 300 keV selenium ions to a dose of 1×10^{15} ions cm^{-2}. There is a good correlation also between these TEM results [10] and the variation of sheet resistivity and damage parameters, χ_{min}, with energy density (Fig. 1), the lowest resistivity and χ_{min} values occurring when the GaAs is defect free and single crystal. The values of χ_{min} are the lowest for selenium implanted material and equal the value for good crystalline GaAs, that is, about 5%. The somewhat higher value of χ_{min} of 8 to 10% for the tin implanted samples is suggested to be due to the segregation of tin atoms to the surface following laser irradiation [7] (Fig. 1). Because of this high concentration of tin, the He^+ beam will tend to suffer more collisions, and hence dechannelling, than it would if the tin were not present. It follows that the selenium atoms do not segregate to the surface and this has been observed by other workers [11].

Fig. 1 shows an excellent correlation between the sheet resistivity and χ_{min} values for the 300 keV implants of tin and selenium, in that the threshold energy density is identical for the two measurement techniques. This threshold energy density corresponds to the transition between regions 1 and 2 of the TEM results (Fig. 5). Thus good electrical properties can be obtained for defective crystalline GaAs. However, the lowest resistivities for the selenium-implanted samples were obtained for defect free crystalline material which corresponds to irradiation with energy densities of about 0.6 to 1.0 J cm^{-2}. The results for tin implants are somewhat different since the resis-

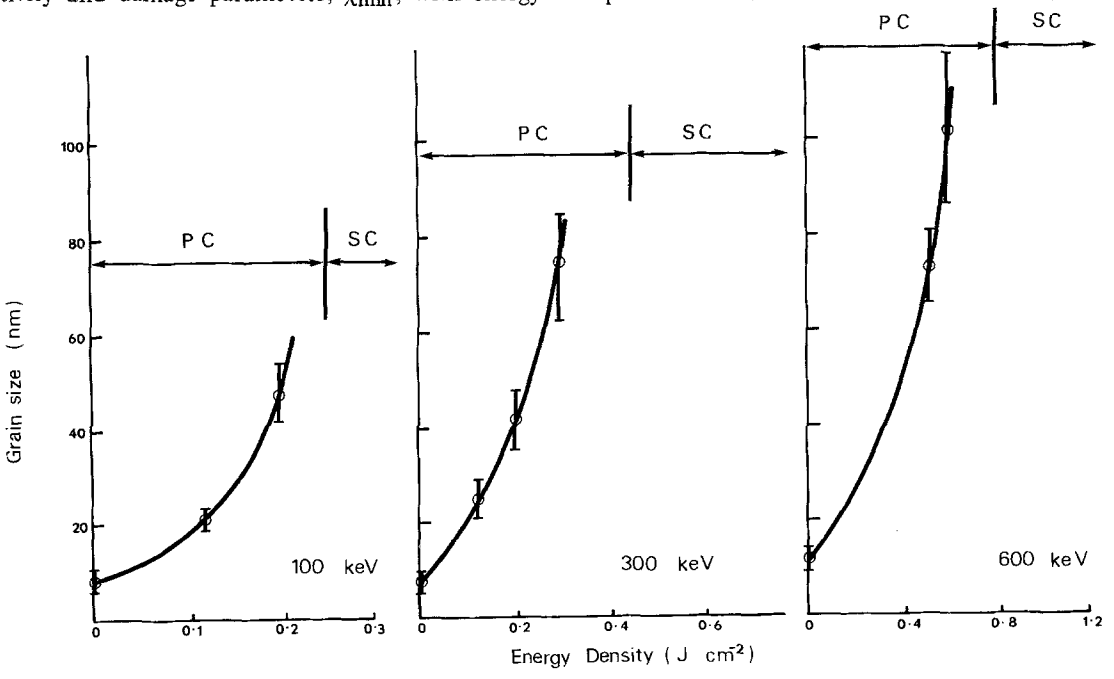

Figure 6 Grain size as a function of energy density for 5×10^{14} Sn^+cm^{-2} implanted into GaAs at ion energies of 100, 300 and 600 keV. PC – polycrystalline GaAs, SC – single crystal GaAs.

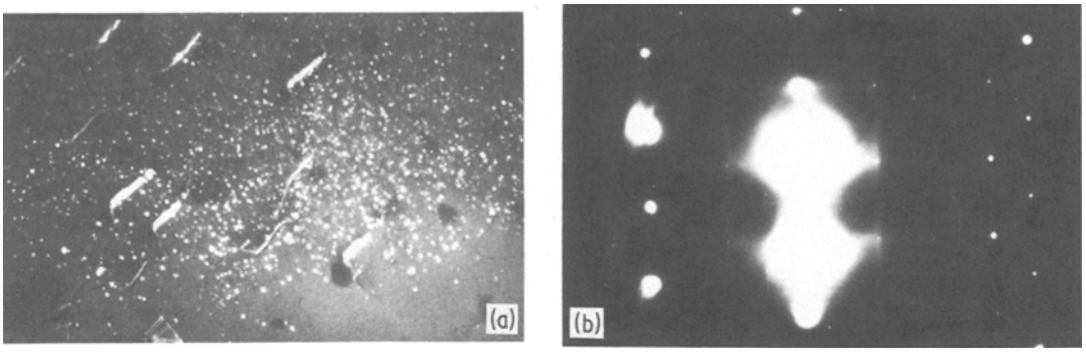

Figure 7 (a) A dark field micrograph of tin implanted and laser annealed GaAs. The energy density was 0.47 J cm^{-2}. Implant conditions as in Fig. 3. (b) Diffraction patterns from the same areas as (a).

tivity rises in the region where good crystalline material was formed, that is at values of 0.6 to 1.0 J cm^{-2} (Fig. 1). This is again thought to be related to the segregation of tin to the surface and to the fact that only a small fraction of the remaining tin dissolved in GaAs is electrically active. Thus, as the energy density increases the quantity of tin segregated to the surface increases [7] and hence the amount of tin remaining which can become electrically active decreases with increasing energy density. Despite the large segregation effect, the precipitation of tin has not been positively observed by TEM although some of the precipitates that contain gallium may, however, also contain tin. Also since not all the precipitate particles have been analysed it may be that some are composed of tin.

We have obtained a good correlation between TEM results where the dose was 5×10^{14} $Sn^{+}cm^{-2}$ and the Rutherford backscattering and sheet resistivity measurements where the dose was 1×10^{15} Sn^{+} cm^{-2}. This is not unreasonable since the threshold energy density is a function of the damage layer thickness which for the above two doses differs by about 10%. Thus, the threshold energy densities for the two doses is likely to differ also by about 10%. Assuming that the melt depth is a linear function of energy density, then from the amorphous layer thicknesses and the threshold energy densities (Figs. 1 and 5) we can conclude that the maximum melt depth in microns is approximately equal to half the energy density in J cm^{-2} for damaged GaAs which is in agreement with theoretical calculations [12]. Thus damaged layers of 0.5 μm in thickness will require about 1 J cm^{-2} for recrystallization but at this energy density decomposition and laser induced damage are becoming a problem, so growth will be imperfect. Another way of saying this is that the energy window does not exist for damaged layers of thickness equal to or greater than about 0.5 μm.

The results presented here together with similar

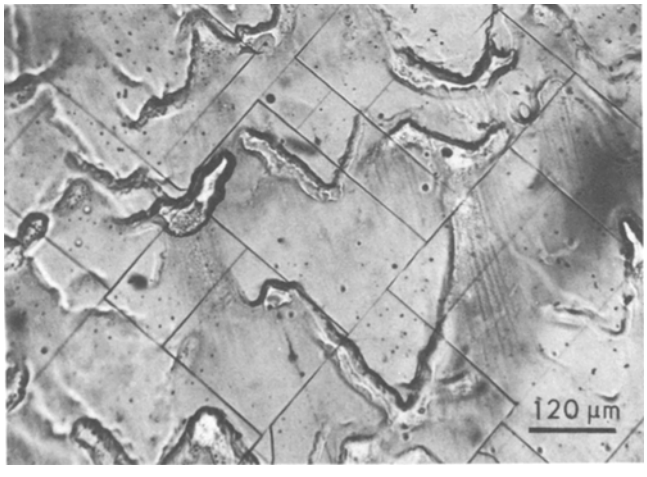

Figure 8 Surface cracks produced in (1 0 0) GaAs by a single 25 nsec pulse from a Q-switched ruby laser. Energy density was 2 J cm^{-2}.

data for zinc implanted GaAs [10] and other published results [11–14] suggest that the threshold energy density is independent of the implanted ion species and so the high threshold energy density measured for tellurium-implanted material [6] is inconsistent with our results and theory [11]. The difference may, therefore, be due to an error in measuring accurately the energy density. Despite this possibility, a correlation between RBS and TEM results was obtained but no electrical properties were reported [3]. Also the magnitude of the energy window was not discussed. Thus in the present study we have obtained a more detailed decription than previous work of the processes occurring as the energy density is raised including the effect on the electrical properties. This work has identified also the problem that thick damage layers may not recrystallize without the laser introducing damage due to the high energy density required. That is, there may be no energy window for the damage layers more than 0.5 μm thick. However, preliminary results suggest that a possible solution to this problem is to irradiate with a number of lower energy density pulses. As the material becomes more crystalline after each pulse, the absorption coefficient decreases and hence the melt depth increases. The choice of energy density is critical since too low a value will never produce the desired end result. Of course the same multipulse process can be used to advantage for thin damaged layers in order to reduce the possibility of decomposition.

5. Conclusions

For the first time a good correlation has been observed between electrical properties, Rutherford backscattering measurements and transmission electron microscopy. Four distinct regions have been identified corresponding to (i) an "amorphous" to polycrystalline transition accompanied by grain growth, (ii) the production of defective single crystal GaAs containing dislocations, (iii) the energy window within which good defect free crystalline GaAs is obtained, but with some surface decomposition and (iv) the onset of gross decomposition and laser induced damage at energy densities of about 1 J cm^{-2}. The best electrical properties are associated with recrystallization at energy densities within the energy window, although with tin implanted samples, results are complicated because of the large segregation of tin to the surface. It is suggested that multiple pulse irradiations at energy densities below the threshold value can produce good electrical properties but with a reduction in both the degree of decomposition and laser induced damage.

Acknowledgements

The authors wish to thank SERC for financial support. They also thank Mr J. E. Mynard and staff of both the Accelerator laboratory and Microstructural Studies Unit of the University of Surrey, for technical assistance.

References

1. B. J. SEALY, *J. Cryst. Growth* **48** (1979) 655.
2. S. S. KULAR, B. J. SEALY, K. G. STEPHENS, D. SADANA and G. R. BOOKER, *Solid State Electron.* **23** (1980) 831.
3. W. F. TSENG, J. W. MAYER, S. U. CAMPISANO, G. FOTI and E. RIMINI, *Appl. Phys. Lett.* **32** (1978) 824.
4. A. G. CULLIS, H. C. WEBBER and N. G. CHEW, *ibid.* **36** (1980) 547.
5. Y. HAYAFUGI, T. YANADA and Y. AOKI, *J. Electrochem. Soc.* **128** (1980) 1975.
6. S. U. CAMPISANO, G. FOTI, E. RIMINI, F. H. EISEN, W. F. TSENG, M. A. NICOLET and J. L. TANDON, *J. Appl. Phys.* **51** (1980) 295.
7. M. H. BADAWI, B. J. SEALY and K. G. STEPHENS, *J. Phys. D: Appl. Phys.* **15** (1982) 507.
8. B. J. SEALY, *Microelectron. J.* **13** (1982) 21.
9. A. G. CULLIS, H. C. WEBBER and P. BAILEY, *J. Phys. E: Sci. Instrum.* **12** (1979) 688.
10. M. HOCKLEY, D. K. SADANA, G. R. BOOKER, N. J. BARRATT and B. J. SEALY, "Microscopy of Semiconducting Materials", Institute of Physics Conference Series No. 60 (Institute of Physics, Bristol, 1981) p. 113.
11. P. A. PIANETTA, C. A. STOLTA and J. L. HANSEN, "Laser and Electron Beam Processing of Materials", edited by C. W. White and P. S. Pearcy (Academic Press, New York, 1980) p. 328.
12. R. F. WOOD, D. H. LOWNDES and N. H. CHRISTIE, "Laser and Electron Beam, Solid Interactions and Material Processing", edited by J. F. Gibbons, L. D. Hess and T. W. Sigmon (North Holland, Amsterdam, 1981) p. 231.
13. Q. KIM, Y. S. PARK, R. S. MASON, T. E. LUKE, R. L. HENGEHOLD and Y. K. YEO, "Laser-Solid Interactions and Laser Processing – 1978", American Institue of Physics Conference Proceedings No. 50, edited by S. D. Ferri, H. J. Leamy and J. M. Poate (American Institute of Physics, 1979) p. 597.
14. R. TSU, J. E. BAGLIN, G. J. LASHER and J. C. TSANG, *Appl. Phys. Lett.* **34** (1979) 153.

Received 18 December 1983
and accepted 16 January 1984